Catalysis Science & Technology

ARTICLE

Tin-palladium supported on alumina as a highly active and selective catalyst for hydrogenation of nitrate in actual groundwater polluted with nitrate

Received 00th January 20xx,
Accepted 00th January 20xx

DOI: 10.1039/x0xx00000x

www.rsc.org/

Jun Hirayama[a,b] and Yuichi Kamiya[b]*

We developed $Sn_{0.5}Pd/Al_2O_3$ showing high activity and high selectivity to gaseous products towards the hydrogenation of NO_3^- with H_2 in aqueous NO_3^- solutions via precise control of the Sn/Pd molar ratio. For the catalyst with the optimum Sn/Pd molar ratio, the surface concentration of adsorbed nitrogen on the Pd sites is thought to be high and that of the adsorbed hydrogen on the Pd sites is thought to be low. This is due to the abundant supply of NO_2^- for the Pd sites and the prompt consumption of adsorbed H on the Pd sites for reduction of the oxidized Sn sites formed by the reduction of NO_3^-, respectively, leading to the high selectivity to gaseous products. Although the catalytic performance of $Sn_{0.5}Pd/Al_2O_3$, like that of $Cu_{0.5}Pd/Al_2O_3$, was lower in groundwater, the decrease for $Sn_{0.5}Pd/Al_2O_3$ was less than that for $Cu_{0.5}Pd/Al_2O_3$. Nitrate in the groundwater polluted with 0.4 mmol dm^{-3} (250 cm^3) of NO_3^- was completely reduced at 298 K in 24 h with a selectivity for gaseous products of around 90% in the presence of 10 mg of $Sn_{0.5}Pd/Al_2O_3$, whereas it took 60 h in the presence of $Cu_{0.5}Pd/Al_2O_3$, and the selectivity for gaseous products was around 75%. However, both catalysts showed comparable high activity and high selectivity in aqueous NO_3^- solutions. When reactions were performed in aqueous NO_3^- solutions containing other anions (Cl^-, SO_4^{2-}, and SiO_x^{n-}) present in the groundwater, Cl^- had the largest negative impact but it had a smaller impact in the presence of $Sn_{0.5}Pd/Al_2O_3$ than it did in the presence of $Cu_{0.5}Pd/Al_2O_3$. On the basis of adsorption isotherms for Cl^- and kinetics analysis of the hydrogenation of NO_3^-, it was concluded that $Sn_{0.5}Pd/Al_2O_3$ had less affinity for Cl^- and a strong affinity for NO_3^- on the Sn sites, leading to its superior catalytic performance in groundwater.

Introduction

Since safe drinking water is necessary for a sustainable society, we must ensure a clean, sustainable water supply. Groundwater is one of the most important water resources owing to its good quality and abundance. However, pollution of groundwater with nitrate (NO_3^-) caused by overuse of agricultural fertilizers, inappropriate disposal of livestock excreta, and leakage of industrial and domestic effluents is now a serious global problem, making it difficult to maintain safe drinking water supplies.[1] Nitrate taken by mouth can be reduced into nitrite (NO_2^-) in the human body and may cause various diseases, including methemoglobinemia, *i.e.*, blue-baby syndrome.[2] Thus, the World Health Organization recommends that the concentration of NO_3^- in drinking water should be below 50 mg dm^{-3}, which corresponds to 0.8 mmol dm^{-3}.[3]

Catalytic hydrogenation of NO_3^- into harmless nitrogen (eqn (1)) in water has been extensively investigated as a promising technology to remediate NO_3^--polluted groundwater[4-42] since Vorlop and Tache found that Cu-Pd/Al_2O_3 showed activity toward the reaction.[4] However, the formation of nitrite (NO_2^-, eqn (2)) and ammonium ion (NH_4^+, eqn (3)) is a critical problem in the catalytic hydrogenation of NO_3^- and should be suppressed to allowable levels, which are 0.1 and 0.5 mg dm^{-3}, respectively.

$$NO_3^- + 5/2H_2 \rightarrow 1/2N_2 + 2H_2O + OH^- \quad (1)$$

$$NO_3^- + H_2 \rightarrow NO_2^- + H_2O \quad (2)$$

$$NO_3^- + 4H_2 \rightarrow NH_4^+ + H_2O + 2OH^- \quad (3)$$

Many studies have dealt with supported Pd-based bimetallic catalysts, on which NO_3^- is reduced into NO_2^- on base basic metal sites, such as Cu, Sn, and In, and then NO_2^- is reduced into final products on the Pd sites.[24,25] Since the Pd sites do not activate NO_3^-, although appropriate base metal ones can, combining Pd with a base metal is essential for catalytic activity towards the reaction. Among Pd-based bimetallic catalysts, Cu-Pd ones have been the most extensively studied because of their high activity and selectivity.[6-18,23,24,27-34] In most studies on Cu-Pd catalysts, the catalytic performances were evaluated in distilled or deionized water, in which nitrate (MNO_3, M = Na or K) was dissolved, and some

[a] Research Fellow of Japan Society for the Promotion of Science (JSPS), 5-3-1 Chiyoda-ku, Tokyo 102-0083, Japan.
[b] Faculty of Environmental Earth Science, Hokkaido University, Nishi 5, Kita 10, Kita-ku, Sapporo 060-0810, Japan. *E-mail:* kamiya@ees.hokudai.ac.jp

† Electronic Supplementary Information (ESI) available: Catalytic performance of $Sn_{0.5}Pd/Al_2O_3$ with different metal loadings for the hydrogenation of NO_3^-. See DOI: 10.1039/x0xx00000x

catalysts with high activity, selectivity, and durability in such reaction solutions have been developed.

Evaluation of the catalytic performances in groundwater is a necessary consideration for practical applications of this catalytic purification technology because coexisting matter in groundwater, including cations, anions, and water-soluble organic compounds, affects the catalytic performance. In some studies, Cu-Pd catalysts have been used for the reaction in actual groundwater, natural water and tap water samples.[23,29–31,36] However, substantial decreases in the performance of the Cu-Pd catalysts have been observed in those water samples, although the catalysts exhibited good performance in distilled or deionized water.[29,31] Pintar et al. have compared the catalytic performance of Cu-Pd/Al_2O_3 in tap water with that in aqueous NO_3^- solutions and pointed out that hydrogen carbonate (HCO_3^-) in tap water causes a decrease in the catalytic performance.[29] We have investigated the effects of ions in reaction solutions on the catalytic performance of Cu-Pd/activated carbon by using aqueous NO_3^- solutions containing cations or anions present in groundwater samples and have shown that Cl^- causes a substantial decrease in the catalytic activity and selectivity towards harmless gaseous products (N_2 and N_2O) in groundwater.[31] Furthermore, we have clarified that poisoning of the Cu sites by Cl^- leads to catalyst deactivation.[31] In addition, Chaplin et al. have reported that the activity and selectivity towards gaseous products for the hydrogenation of NO_3^- over Cu-Pd/Al_2O_3 decreases in the presence of Cl^-.[32] Sulfate ion and its reduced products, including SO_3^{2-} and HS^-, formed under the reaction conditions, greatly decrease the reaction rate for NO_3^- reduction over supported Cu-Pd catalysts.[32,37]

Pd-based bimetallic catalysts, other than Cu-Pd, including Sn-Pd[19-24,27-29,34,35] and In-Pd[24-28,34] show activity towards the hydrogenation of NO_3^-. The base metal sites in these catalysts have different affinities for coexisting ions in water from those of the Cu sites in Cu-Pd catalysts, and thus, the catalysts have strong potential to deliver superior performance in groundwater than Cu-Pd catalysts do. In fact, Palomares et al. have found that Sn-Pd/Al_2O_3 has lower selectivity for NH_4^+ in actual groundwater polluted with NO_3^- than Cu-Pd/Al_2O_3 does (20–40% and 40–60% for Sn-Pd/Al_2O_3 and Cu-Pd/Al_2O_3, respectively), whereas both catalysts had similar activities.[30,36] Sn-Pd/Al_2O_3 is applicable to the purification of actual groundwater, although the selectivity towards gaseous products is still low. In other words, it is too low to meet allowable levels for drinking. In addition, the effects of co-existing ions in the water on the catalytic performances of Sn-Pd catalysts must be studied in detail to develop catalysts with good activity and selectivity in groundwater.

In the present study, we developed highly active and selective Sn-Pd bimetal supported on Al_2O_3 (SnPd/Al_2O_3) for the hydrogenation of NO_3^- in water by precisely controlling the Sn/Pd ratio and used it for the treatment of an actual groundwater sample polluted with NO_3^-. The catalytic performance of SnPd/Al_2O_3 was compared with that of CuPd/Al_2O_3 in groundwater as well as in aqueous NO_3^- solutions to demonstrate superiority and high tolerance of SnPd/Al_2O_3 in the groundwater sample. In addition, we discuss reasons for the superiority and high tolerance of SnPd/Al_2O_3 in the groundwater via kinetic analysis and measurements of adsorption isotherms for anions present in the groundwater and by comparing its abilities with those of CuPd/Al_2O_3.

Experimental

Preparation of catalysts

Sn and Pd supported on γ-Al_2O_3 (AEROSIL, Alu C) was prepared by using incipient wetness impregnation. Powdered Al_2O_3 was heated in air at 523 K for 4 h before use. An aqueous solution of $PdCl_2$ (0.112 mol dm^{-3}, Wako Pure Chemical Industries) was dropped onto the Al_2O_3, and then the resulting wet solid was dried in air at 373 K overnight, followed by calcination in air at 523 K for 3 h. An aqueous solution of $SnCl_2$ (0.172 mol dm^{-3}), prepared using $SnCl_2{\cdot}2H_2O$ (Wako Pure Chemical Industries), was dropped onto the resulting solid, and then the wet solid was dried in air at 373 K overnight, followed by calcination in air at 523 K for 3 h. The total loading amount of Sn and Pd was fixed at 6.5 wt% while the Sn/Pd molar ratio was changed. The obtained catalysts are denoted as Sn_nPd/Al_2O_3, where n represents the Sn/Pd ratio. In this study, Sn_nPd/Al_2O_3 catalysts with n = 0.1, 0.5, 0.75, 1, 2, 3, and 5 were prepared. In addition, Sn/Al_2O_3 (2.3 wt% Sn) and Pd/Al_2O_3 (4.2 wt% Pd) were prepared as references.

CuPd/Al_2O_3 was prepared by using a procedure similar to that for SnPd/Al_2O_3. An aqueous solution of $Cu(NO_3)_2$ (0.161 mol dm^{-3}), prepared using $Cu(NO_3)_2{\cdot}3H_2O$ (Kanto Chemical Industries), was dropped onto the Pd/Al_2O_3, and then the wet solid was dried and calcined in air at 523 K for 3 h. The loading amounts of Cu and Pd were 1.3 wt% and 4.2 wt%, respectively. The Cu/Pd molar ratio was 0.5, which is denoted as $Cu_{0.5}Pd/Al_2O_3$.

Just before the catalytic hydrogenation of NO_3^- in water, the catalyst was reduced with $NaBH_4$ (Wako Pure Chemical Industries). $NaBH_4$ (molar ratio of $NaBH_4$/(Sn+Pd) = 10) was added to an aqueous suspension (30 cm^3) in which Sn_nPd/Al_2O_3 was dispersed, and the suspension was stirred at room temperature for 30 min. The catalyst powder was filtered, washed with distilled water (ca. 200 cm^3), and then used in the reactions. The reduction of CuPd/Al_2O_3 was performed by using a procedure similar to that for SnPd/Al_2O_3.

Characterization

Powder X-ray diffraction (XRD) was performed using an X-ray diffractometer (Rigaku Mini Flex) with Cu Kα radiation (λ = 0.154 nm). The crystallite size of the Pd was determined by using Scherrer's equation with a diffraction line at $2\theta = 40°$. Transmission electron microscopy (TEM) images were obtained with a JEM-2100F (JEOL). The particle sizes of the Pd metal were estimated from the amounts of adsorbed CO at 323 K, which were measured on a BEL-CAT instrument (BEL Japan Inc). The stoichiometry of CO to metal was assumed to be two.[43]

Component analysis of groundwater

Groundwater polluted with NO_3^- was obtained from a well in Sapporo, Hokkaido, Japan (denoted as GW). The concentrations of the anions and cations in the GW were determined by using two ion-chromatographs (Tosoh Co., IC-2001). A column containing an

Table 1 Concentrations of the components in the groundwater used in this study.

Component	Concentration/mmol dm^{-3}
NO_3^-	0.4
Cl^-	1.0
SO_4^{2-}	0.5
SiO_x^{n-}	0.3
Na^+	1.0
K^+	0.1
Mg^{2+}	1.0
Ca^{2+}	0.5
TOC[a]	1.2

[a] Total organic carbon (mg dm^{-3})

anion-exchange resin (TSK gel Super IC-AZ, Tosoh) and an aqueous solution of $NaHCO_3$ (2.9 mmol dm^{-3}) and Na_2CO_3 (3.1 mmol dm^{-3}) were used as stationary and mobile phases, respectively, for anion analysis. For cation analysis, a column containing a cation-exchange resin (TSK gel IC-Cation 1/2 HR, Tosoh) and an aqueous solution of methanesulfonic acid (2.2 mmol dm^{-3}) and 18-crown-6 (1.0 mmol dm^{-3}) were used as stationary and mobile phases, respectively.

The concentrations of the Si species in the GW were measured by using inductively coupled plasma atomic emission spectroscopy (ICP-AES) on a Shimadzu ICPS-7000. The Si species present in the GW were anionic compounds (silicate ion, SiO_x^{n-}) because no Si was detected in the GW treated with an anion-exchange resin. The amounts of organic compounds in the groundwater were measured by using a total organic carbon (TOC) analyzer (Shimadzu Inc, TOC-5000A). The components contained in the groundwater (GW) are listed in Table 1.

Reaction solutions

Aqueous NO_3^- solutions with different concentrations (0.4, 0.8, and 1.6 mmol dm^{-3}) were prepared by dissolving KNO_3 (Wako Pure Chemical Industries) in distilled water and are denoted as KNO_3-aq(x), where x represents the concentration of NO_3^- (x = 0.4, 0.8, or 1.6). KNO_3-aq(0.4) and KNO_3-aq(0.8) were used for comparison of the catalytic performances with that in GW and for optimization of the Sn/Pd molar ratio of Sn_nPd/Al_2O_3, respectively. For kinetic analysis, KNO_3-aq(1.6) was used in addition to KNO_3-aq(0.4) and KNO_3-aq(0.8).

Aqueous NO_3^- solutions containing Cl^-, SO_4^{2-}, and SiO_3^{2-} with different concentrations were prepared by adding KCl (Wako Pure Chemical Industries), K_2SO_4 (Wako Pure Chemical Industries), and K_2SiO_3 (Wako Pure Chemical Industries), respectively, to KNO_3-aq(0.8).

Catalytic hydrogenation of NO_3^- with H_2

Catalytic hydrogenation of NO_3^- in water was carried out in a batch reactor at 298 K. The reaction solution (250 cm^3) containing 10 mg of Sn_nPd/Al_2O_3 was purged with a stream of He (30 cm^3 min^{-1}) for 30 min. Then the gas was changed to a mixture of H_2 (0.5 atm) and CO_2 (0.5 atm) to start the reaction. A small portion of the reaction solution was periodically withdrawn and analyzed by using ion-chromatographs to determine the concentrations of NO_3^-, NO_2^-, and NH_4^+.

The reaction rate for NO_3^- reduction was estimated from the data where the decrease in the concentration of NO_3^- occurred almost linearly with the reaction time. The selectivities towards NO_2^- and NH_4^+ were calculated by using eqn (4).

$$\textbf{Selectivity to } NO_2^- \textbf{ (or } NH_4^+\textbf{)} = \frac{\textbf{Concentration of formed } NO_2^- \textbf{ (or } NH_4^+\textbf{)}}{\textbf{Concentration of consumed } NO_3^-} \quad (4)$$

Because gaseous products were not analyzed in this study, the selectivities towards them were calculated by subtracting the selectivities to NO_2^- and NH_4^+ from 100%.

Adsorption isotherms of Cl^- in water

Adsorption isotherms of Cl^- in water for Al_2O_3, Sn/Al_2O_3, and Cu/Al_2O_3 were measured at 303 K as follows. Sample powder (30 mg) was added to an aqueous Cl^- solution (10 cm^3) prepared by adding different amounts of KCl (concentration range = 0.2 – 3.2 mmol dm^{-3}), and then the suspension was heated at 303 K with stirring. After 24 h, the solid was filtered off, and the concentration of Cl^- in the filtrate was determined using an ion-chromatograph. The amount of adsorbed Cl^- was calculated by subtracting the concentrations after 24 h from the initial one.

Results and discussion

Effects of Sn/Pd ratio on the hydrogenation of NO_3^- over Sn_nPd/Al_2O_3

Figure 1 shows the dependence of NO_3^--decomposition rate (catalytic activity) and selectivities in the hydrogenation of NO_3^- with H_2 in KNO_3-aq(0.8) on the Sn/Pd ratio over Sn_nPd/Al_2O_3. Since the total loading amounts of Sn and Pd were fixed at 6.5 wt%, when the Sn/Pd ratio was larger, the loading amount of Pd was lower, whereas that of Sn was higher. The catalytic activity of Sn_nPd/Al_2O_3 drastically changed with the Sn/Pd ratio. Pd alone supported on Al_2O_3 showed negligible activity for the reaction. Modification of Pd/Al_2O_3 with a small amount of Sn dramatically enhanced the NO_3^--decomposition rate, and the rate reached a maximum at Sn/Pd = 0.1. Excess Sn decreased the catalytic activity, and Sn/Al_2O_3 was completely inactive for the reaction.

The selectivities changed depending on the Sn/Pd ratio, although the changes were not significant. The catalyst with Sn/Pd = 0.5 ($Sn_{0.5}Pd/Al_2O_3$) showed the highest selectivity towards gaseous products (> 99%) and the lowest selectivity towards undesirable NH_4^+. Only negligible NO_2^- formed regardless of the Sn/Pd ratio.

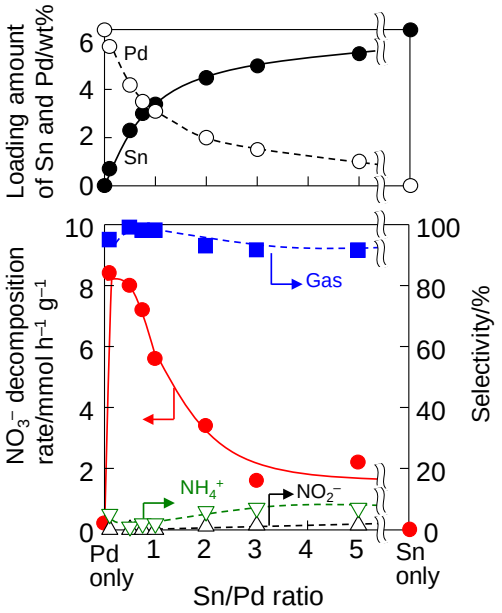

Figure 1 Dependences of the NO_3^- decomposition rate (●) and selectivities for gaseous nitrogen compounds (■), NH_4^+ (▽), and NO_2^- (△) on the Sn/Pd ratio at around 30% NO_3^- conversion over Sn_nPd/Al_2O_3 for the catalytic hydrogenation of NO_3^- in aqueous NO_3^- solutions (KNO_3-aq(0.8)). Reaction conditions: catalyst weight, 10 mg; reactant NO_3^- (from KNO_3), 0.8 mmol dm^{-3}; volume of reaction solution, 250 cm^3; gas composition, H_2/CO_2 = 1/1; gas flow rate, 30 cm^3 min^{-1}; and reaction temperature, 298 K.

Thus, we concluded that $Sn_{0.5}Pd/Al_2O_3$ was the best catalyst in terms of activity as well as selectivity. In a separate experiment, we conducted the catalytic hydrogenation of NO_3^- using a physical mixture of 10 mg of Sn/Al_2O_3 (2.3 wt% Sn) and 10 mg of Pd/Al_2O_3 (4.2 wt% Pd), in which the amounts of Sn and Pd in the reactor were the same as those for the ordinary $Sn_{0.5}Pd/Al_2O_3$. The NO_3^--decomposition rate was less than 0.1 mmol h^{-1} g^{-1}, which was ≤ 1% of the rate of the ordinary $Sn_{0.5}Pd/Al_2O_3$, indicating that Pd must be adjacent to Sn on Al_2O_3 for the reaction to proceed.

The changes in the catalytic performance with the Sn/Pd ratio suggest that the Sn/Pd ratio affects the structure of the SnPd particles. Hence, we examined the structure of the SnPd particles in Sn_nPd/Al_2O_3 by using powder X-ray diffraction (XRD) and transmission electron microscopy (TEM). Figure 2 shows XRD patterns of Sn_nPd/Al_2O_3 with different Sn/Pd ratios. Since the diffraction lines of Pd metal overlapped those of Al_2O_3 (data not shown), the XRD patterns were obtained by subtracting that of Al_2O_3 from that of each Sn_nPd/Al_2O_3. Two diffraction lines for Pd/Al_2O_3 were observed at 2θ = 40° and 46°, which represent (111) and (200) of crystalline Pd with a face-centered cubic (fcc) structure. The diffraction line due to Pd (111) was observed for the catalysts with Sn/Pd < 2 (Fig. 2b and c). No diffraction lines were observed for the catalysts with a high Sn/Pd ratio due to the low loading

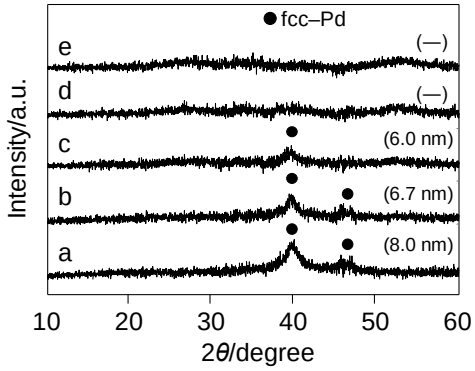

Figure 2 Powder XRD patterns of Pd/Al_2O_3, Sn/Al_2O_3, and Sn_nPd/Al_2O_3. The XRD patterns shown in the figure were obtained by subtracting that of Al_2O_3 from that of each catalyst. (a) Pd/Al_2O_3, (b) $Sn_{0.5}Pd/Al_2O_3$, (c) Sn_2Pd/Al_2O_3, (d) Sn_5Pd/Al_2O_3, and (e) Sn/Al_2O_3. Figures in parenthesis are crystallite sizes of Pd estimated by applying Scherrer's equation on the Pd(111) diffraction line at 2θ = 40°.

amount of Pd, as mentioned above. In contrast, no diffraction lines for crystalline Sn or tin oxides (SnO_x) were observed regardless of the Sn/Pd ratio. It should be noted that the diffraction lines were not shifted due to crystalline Pd for any Sn/Pd ratio, indicating that a SnPd alloy did not form. Thus, the absence of diffraction lines for Sn and SnO_x suggests the formation of fine Sn particles (or SnO_x) undetectable by using XRD or amorphous Sn (or SnO_x). As mentioned above, since Sn and Pd must be adjacent on Al_2O_3 for the reaction, Sn (or SnO_x) may have deposited on Pd particles, or was located very close to the Pd particles on Al_2O_3.

The crystallite size of Pd in Pd/Al_2O_3 was estimated from the Pd (111) diffraction line to be 8.0 nm by applying Scherrer's equation. The crystallite size was roughly consistent with the average particle size of Pd estimated from the TEM image (Fig. 3(a)) and that from CO chemisorption (d = 5.6 nm). The crystallite sizes of Pd were 6.7

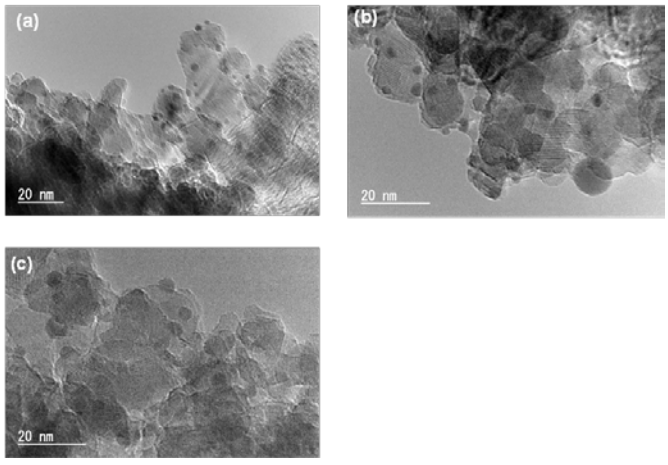

Figure 3 TEM images of (a) Pd/Al_2O_3, (b) $Sn_{0.5}Pd/Al_2O_3$, and (c) Sn_3Pd/Al_2O_3.

and 6.0 nm in $Sn_{0.5}Pd/Al_2O_3$ and Sn_2Pd/Al_2O_3, respectively (Fig. 2b and 2c). The decrease in the crystallite size of Pd is thought to be due to the low amount of Pd. However, the sizes of the metal particles observed in the TEM images for $Sn_{0.5}Pd/Al_2O_3$ and Sn_3Pd/Al_2O_3 were larger than those for Pd/Al_2O_3. Thus, it is more plausible that Sn (or SnO_x) deposits on the Pd particles, forming a structure with a Pd core and Sn shell in Sn_nPd/Al_2O_3.

The following reaction mechanism for the hydrogenation of NO_3^- over supported SnPd catalysts has been proposed (Scheme 1) [24,25]: The reaction proceeds consecutively through NO_2^- as an intermediate. The conversion of NO_3^- to NO_2^- is a rate-determining step[8,16] and proceeds over SnPd bimetallic sites. Metallic Sn or low-valent Sn^{n+} reduces NO_3^- to NO_2^- and consequently Sn or low-valent Sn^{n+} is oxidized. The oxidized Sn species is then reduced with hydrogen activated on the Pd sites, affording the original Sn species. The intermediate NO_2^- is then reduced over the Pd site to the final products (N_2, N_2O and NH_4^+), and Sn is not involved in the reaction. Thus, we believe that the high catalytic activity for the catalysts with the Sn/Pd ratio in the range of 0.1–0.5 is due to the large number of SnPd bimetallic sites on the catalysts. Excess Sn may cover the surface of Pd particles, resulting in the decrease in the catalytic activity.

Yoshinaga *et al.* have shown that the selectivity to gaseous products (N_2 and N_2O) increases with an increase in the size of the Pd particles for the hydrogenation of NO_2^- over Pd/active carbon.[12] On the basis of the results, they propose that the gaseous products form mainly on the terrace Pd sites with low hydrogenation-ability and that NH_4^+ forms in the edge and corner Pd sites due to high hydrogenation-ability. However, in the present study, the size of the Pd particles was not a critical factor for the selectivity. In a separate experiment, we prepared 1.0 wt% $Sn_{0.5}Pd/Al_2O_3$, for which the total metal loading was about one-seventh of that for the ordinary 6.5 wt% $Sn_{0.5}Pd/Al_2O_3$ but the Sn/Pd ratio (Sn/Pd = 0.5) was the same. Although it was impossible to determine the Pd particle size for 1.0 wt% $Sn_{0.5}Pd/Al_2O_3$ because no diffraction line due to a fcc Pd particle was detected in the XRD pattern, we thought that the particle size for 1.0 wt% $Sn_{0.5}Pd/Al_2O_3$ was smaller than that for the ordinary $Sn_{0.5}Pd/Al_2O_3$. However, the selectivity to gaseous products for 1.0 wt% $Sn_{0.5}Pd/Al_2O_3$ was almost the same as that of ordinary $Sn_{0.5}Pd/Al_2O_3$, whereas the NO_3^--decomposition rate was much lower than that of the ordinary one (ESI). Therefore, the high selectivity to gas products for $Sn_{0.5}Pd/Al_2O_3$ was not due to the formation of large Pd particles.

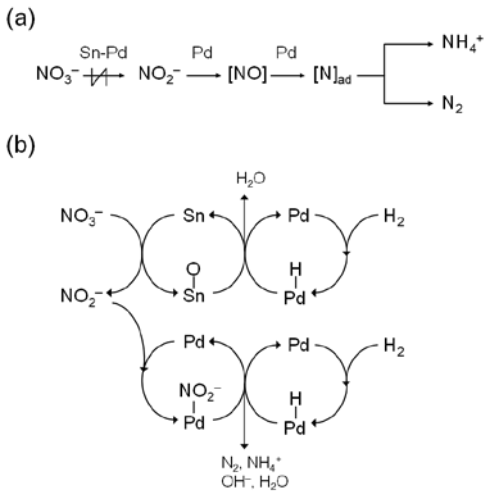

Scheme 1 (a) Reaction pathway for the catalytic hydrogenation of NO_3^- and (b) reaction mechanism over $SnPd/Al_2O_3$.

Another reason for the high selectivity over $Sn_{0.5}Pd/Al_2O_3$ is the concentrations of adsorbed nitrogen ($[N_{ad}]$) and hydrogen ($[H_{ad}]$) on the Pd sites. Since the reaction of N_{ad} with H_{ad} affords NH_4^+, NH_4^+ likely forms when $[N_{ad}]$ is low or $[H_{ad}]$ is high under the reaction conditions. On the other hand, two N_{ad} are necessary for N_2 and thus, high $[N_{ad}]$ or low $[H_{ad}]$ leads to high selectivity to N_2. On Sn_nPd/Al_2O_3 catalysts with Sn/Pd < 1, which showed a high NO_3^--decomposition rate, $[N_{ad}]$ would be high because the rate of NO_3^- reduction is fast. In other words, the supply of NO_2^- to the Pd sites was high. In addition, $[H_{ad}]$ would be low on such catalysts due to the prompt consumption of H_{ad} on the Pd sites to reduce the oxidized Sn species. Therefore, the catalysts with Sn/Pd < 1 showed a high selectivity to gaseous products as well as a high catalytic activity.

Catalytic performance of $Sn_{0.5}Pd/Al_2O_3$ in actual groundwater and a comparison with $Cu_{0.5}Pd/Al_2O_3$

Figure 4a shows time courses for the hydrogenation of NO_3^- in actual groundwater (GW) over $Sn_{0.5}Pd/Al_2O_3$ and $Cu_{0.5}Pd/Al_2O_3$. As a comparison, those in aqueous NO_3^- solution (KNO_3-aq(0.4)) are given in Fig. 4b. The concentrations of NO_3^- in both reaction solutions were the same. It is noted that the catalytic activity of $Sn_{0.5}Pd/Al_2O_3$ is higher than that of $Cu_{0.5}Pd/Al_2O_3$ in the aqueous NO_3^- solution (Fig. 4b). 100% conversion was obtained at 2 h over $Sn_{0.5}Pd/Al_2O_3$, whereas it took 3 h for $Cu_{0.5}Pd/Al_2O_3$.

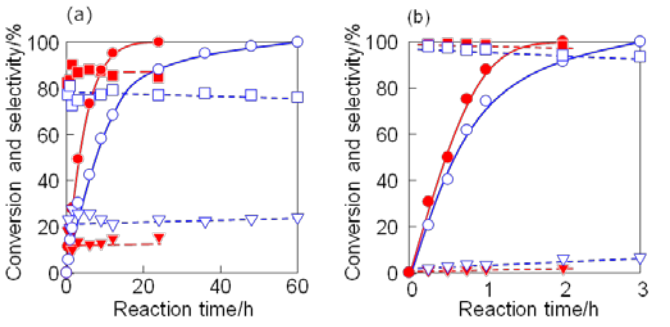

Figure 4 Time courses for conversion of NO_3^- (●, ○) and selectivities for gaseous nitrogen compounds (■, □) and NH_4^+ (▼, ▽) over $Sn_{0.5}Pd/Al_2O_3$ (closed symbol in red) and $Cu_{0.5}Pd/Al_2O_3$ (open symbol in blue) for catalytic hydrogenation of NO_3^- in (a) groundwater (GW) and (b) an aqueous NO_3^- solution (KNO_3-aq(0.4)). Reaction conditions: catalyst weight, 10 mg; reactant NO_3^-, 0.4 mmol dm^{-3}; volume of reaction solution, 250 cm^3; gas composition, H_2:CO_2 = 1/1; gas flow rate, 30 cm^3 min^{-1}; and reaction temperature, 298 K.

For the reactions in GW, NO_3^- completely decomposed over both catalysts, but longer times than those in the aqueous NO_3^- solution were necessary: 24 h and 60 h for $Sn_{0.5}Pd/Al_2O_3$ and $Cu_{0.5}Pd/Al_2O_3$, respectively. The catalysts were significantly deactivated in GW regardless of the base metals. However, $Sn_{0.5}Pd/Al_2O_3$ was more active in GW than $Cu_{0.5}Pd/Al_2O_3$ was. In fact, the NO_3^--decomposition rates in GW were about one-fifth of those in the aqueous NO_3^- solution for $Sn_{0.5}Pd/Al_2O_3$, and they were about one-seventh of those for $Cu_{0.5}Pd/Al_2O_3$. In addition, it should be noted that the decrease in the NO_3^--decomposition rate was quite notable when the conversion over $Cu_{0.5}Pd/Al_2O_3$ was greater than 80%. The concentrations of other ions, like Cl^-, SO_4^{2-}, and SiO_x^{n-}, in the reaction solution basically did not change under the reaction conditions, and their concentrations became high relative to NO_3^- in the high NO_3^- conversion region. Thus, the adverse effects of the other anions became significant.

As shown in Fig. 4, the selectivity for $Sn_{0.5}Pd/Al_2O_3$ to gaseous products was about 99% in aqueous NO_3^- solutions but decreased to around 90% in GW. Although $Cu_{0.5}Pd/Al_2O_3$ showed high selectivity to gaseous products similar to $Sn_{0.5}Pd/Al_2O_3$ in the aqueous NO_3^- solution, the selectivity over $Cu_{0.5}Pd/Al_2O_3$ in GW was 75%. The decrease in the selectivity to gaseous products in GW is due to the kinetics involving N_{ad} and H_{ad} as with the changes in the selectivity with the Sn/Pd ratio. In GW, the NO_3^--decomposition rate was lower. The decrease in the NO_3^--decomposition rate caused low $[N]_{ad}$ and high $[H]_{ad}$, leading to a decrease in the selectivity to gaseous products. Since the NO_3^--decomposition rate in GW was slower for $Cu_{0.5}Pd/Al_2O_3$ than it was for $Sn_{0.5}Pd/Al_2O_3$, the decrease in the selectivity to gaseous products was more significant for the catalyst.

In conclusion, the catalytic performances were lower in GW, but the activity and selectivity for $Sn_{0.5}Pd/Al_2O_3$ were better than those for $Cu_{0.5}Pd/Al_2O_3$. In other words, $Sn_{0.5}Pd/Al_2O_3$ has a high tolerance in GW, which is important for the purification of real groundwater. The reason for the high tolerance of $Sn_{0.5}Pd/Al_2O_3$ is discussed in detail in the following section.

Effects of anions in water samples on the catalytic performance

Since GW contained various compounds (Table 1), those must have a negative impact on the catalytic performances, although the degree of their impact depends on the base metals in the Pd-based bimetallic catalysts. We have previously reported that coexisting cations in GW, including Na^+, K^+, Ca^{2+} and Mg^{2+}, do not affect the catalytic performance of the supported Cu-Pd catalyst for the hydrogenation of NO_3^-, whereas Cl^- decreased the catalytic performance.[31] In a previous study, we showed that coexisting cations in GW did not affect the catalytic performance of Sn-Pd/Al_2O_3, whereas anions decreased it.[34] Hence, in this study, we systematically investigated the influence of Cl^-, SO_4^{2-}, and SiO_x^{n-}, which were the anions present in GW, on the catalytic performances of $Sn_{0.5}Pd/Al_2O_3$ as well as $Cu_{0.5}Pd/Al_2O_3$.

Figure 5 shows the decomposition rate of NO_3^- and selectivities for the hydrogenation of NO_3^- over $Sn_{0.5}Pd/Al_2O_3$ and $Cu_{0.5}Pd/Al_2O_3$ in aqueous NO_3^- solutions containing different concentrations of Cl^-, SO_4^{2-}, or SiO_3^{2-}. The decrease in the catalytic performance and

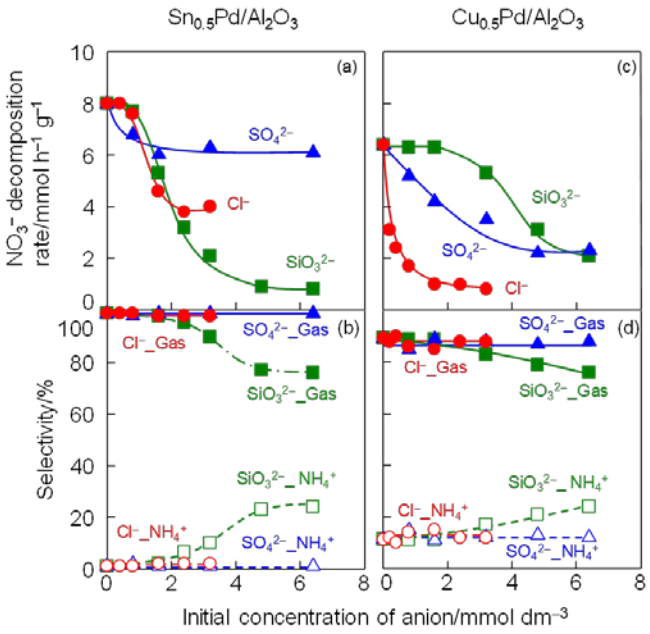

Figure 5 Effects of Cl^-, SO_4^{2-}, and SiO_3^{2-} in water on the catalytic performances of $Sn_{0.5}Pd/Al_2O_3$ and $Cu_{0.5}Pd/Al_2O_3$ for catalytic hydrogenation of NO_3^- with H_2 in water. (a) and (c) NO_3^- decomposition rate and (b) and (d) selectivities to gas (closed symbol) and NH_4^+ (open symbol) at around 30% NO_3^- conversion. Left and right figures are the data for $Sn_{0.5}Pd/Al_2O_3$ and $Cu_{0.5}Pd/Al_2O_3$, respectively. Reaction conditions: catalyst weight, 10–50 mg; reactant NO_3^- (from KNO_3), 0.8 mmol dm^{-3}; volume of reaction solution, 250 cm^3; gas composition, H_2/CO_2 = 1/1; gas flow rate, 30 cm^3 min^{-1}; and reaction temperature, 298 K.

changes in the behavior in relation to the concentrations were different depending on the anions and the catalysts. In the case of $Sn_{0.5}Pd/Al_2O_3$ (Fig. 5a and 5b), the NO_3^--decomposition rates were slower in the presence of SO_4^{2-} even at low concentration but were nearly constant when the concentration was more than 0.8 mmol dm^{-3}. The presence of SO_4^{2-} did not change the selectivity even at high concentrations. On the other hand, low concentrations of Cl^- and SiO_3^{2-} (< 0.8 mmol dm^{-3}) did not affect the decomposition rates of NO_3^- and selectivity. However, the NO_3^--decomposition rates drastically decreased when the concentrations exceeded 1.6 mmol dm^{-3}. In addition, Cl^- and SiO_3^{2-} reduced the NO_3^--decomposition rates much more than SO_4^{2-} did. The NO_3^--decomposition rate at high concentration of Cl^- (> 2.4 mmol dm^{-3}) was only half of that without any coexisting anions. The adverse effects of SiO_3^{2-} were more severe, and the decomposition rate decreased to 0.8 mmol h^{-1} g^{-1}, which was only one-tenth of that without any coexisting anions, and the selectivity to gaseous products decreased with an increase in the concentration of SiO_3^{2-}.

For $Cu_{0.5}Pd/Al_2O_3$ (Fig. 5c and 5d), the NO_3^--decomposition rate decreased in the presence of other anions. The impacts of these anions on the catalytic activity of $Cu_{0.5}Pd/Al_2O_3$ differed according to the kind of anions. The negative impact of Cl^- was the largest among the three, and a substantial decrease in the NO_3^--decomposition rate was observed even at low concentrations. The NO_3^--decomposition rate with a concentration of Cl^- more than 1.6

mmol dm^{-3} was 1.1 mmol h^{-1} g^{-1}, which was only one-sixth of that without any coexisting anions. In contrast to $Sn_{0.5}Pd/Al_2O_3$, SO_4^{2-} had a large negative impact on the NO_3^--decomposition rate for $Cu_{0.5}Pd/Al_2O_3$. The NO_3^--decomposition rate was constant (2.2 mmol h^{-1} g^{-1}) when the concentration of SO_4^{2-} was more than 4.8 mmol dm^{-3}. Low concentrations of SiO_3^{2-} did not affect the catalytic performance of $Cu_{0.5}Pd/Al_2O_3$, similar to $Sn_{0.5}Pd/Al_2O_3$, whereas the activity and selectivity to gaseous products were lower in the presence of high concentrations of SiO_3^{2-}.

The concentrations of Cl^-, SO_4^{2-}, and SiO_x^{n-} in GW were 1.0, 0.5, and 0.3 mmol dm^{-3}, respectively (Table 1). Applying these concentrations to the catalytic data in Fig. 5 affords two conclusions: the adverse impact of Cl^- in GW is the largest among the three anions, and Cl^- has less of an effect on the performance of $Sn_{0.5}Pd/Al_2O_3$ than it does on that of $Cu_{0.5}Pd/Al_2O_3$. Therefore, we concluded that the superior catalytic performance of $Sn_{0.5}Pd/Al_2O_3$ in GW was mainly due to the high tolerance to Cl^-.

Since the reduction of NO_3^- to NO_2^- on the base metal site (Sn or Cu) is the rate-limiting step, as mentioned above, Cl^- adsorption on these base metal sites probably competes with NO_3^- adsorption. To determine the affinity of the Sn and Cu sites for Cl^-, we tried to acquire adsorption isotherms of Cl^- for $Sn_{0.5}Pd/Al_2O_3$ and $Cu_{0.5}Pd/Al_2O_3$. However, it was impossible because the amount of adsorbed Cl^- on the Al_2O_3 support was too large to determine the difference in the affinities; i.e., no difference was observed in the adsorption isotherms of Cl^- between $Sn_{0.5}Pd/Al_2O_3$ and $Cu_{0.5}Pd/Al_2O_3$. Thus, to determine the adsorption behavior on these base metal sites for Cl^-, we prepared 30.0 wt% Sn/Al_2O_3 and 16.1 wt% Cu/Al_2O_3, for which the loading amounts in mmol g^{-1} were the same (2.53 mmol g^{-1}), and acquired the adsorption isotherms of Cl^-. Figure 6 shows the adsorption isotherms of Cl^- for Sn/Al_2O_3, Cu/Al_2O_3, and Al_2O_3. Regardless of the samples, the adsorption amounts increased with an increase in the equilibrium concentrations (C_e).

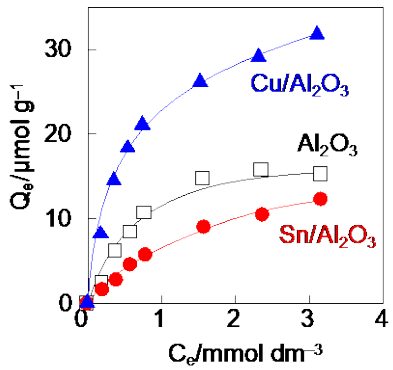

Figure 6 Adsorption isotherms of Cl^- for Sn/Al_2O_3 (●), Cu/Al_2O_3 (▲), and Al_2O_3 (□). Adsorption conditions: weight of adsorbent, 30 mg; temperature, 303 K; volume of solution, 10 cm^3; and adsorption time, 24 h.

Table 2 Langmuir parameters for Cl^- adsorptions on Sn/Al_2O_3, Cu/Al_2O_3, and Al_2O_3.

Absorbent	Q_m/ μmol g^{-1}	K_L/ cm^3 μmol^{-1}	R^2
Sn/Al_2O_3[a]	19.8	0.5	0.99
Cu/Al_2O_3[b]	36.0	1.8	1.00
Al_2O_3	19.4	1.5	0.98

Adsorption conditions: weight of adsorbent, 30 mg; temperature, 303 K; volume of solution, 10 cm^3; and adsorption time, 24 h.

[a] 30.0 wt% Sn/Al_2O_3.

[b] 16.1 wt% Cu/Al_2O_3.

To evaluate the affinity for Cl^- quantitatively, the Langmuir adsorption isotherm equation (eqn (5)) was applied to the isotherms.

$$\frac{C_e}{Q_e} = \frac{C_e}{Q_m} + \frac{1}{K_L Q_m} \quad (5)$$

In eqn (5), Q_e and Q_m are adsorption amount of Cl^- at each equilibrium concentration and the maximum adsorption capacity, respectively, and K_L is an adsorption constant. In Table 2, Q_m and K_L values are summarized. K_L for Sn/Al_2O_3 (0.5 cm^3 μmol^{-1}) was one-third or less of that for Cu/Al_2O_3 (1.8 cm^3 μmol^{-1}). In addition, Q_m for Sn/Al_2O_3 was almost the same as that for the Al_2O_3 support itself and about half of that for Cu/Al_2O_3 (36.0 μmol g^{-1}). These results clearly indicate that the affinity of the Sn sites for Cl^- is lower than that of the Cu sites. In other words, the weak affinity of the Sn sites for Cl^- is the reason for the high tolerance of $Sn_{0.5}Pd/Al_2O_3$ to Cl^- in water.

In addition, the strong affinity of the Sn sites for NO_3^- is another reason for the high tolerance of $Sn_{0.5}Pd/Al_2O_3$ against Cl^- in the hydrogenation of NO_3^- in GW especially in high conversion regions. In Fig. 7, the logarithm of the NO_3^--decomposition rates for the hydrogenation of NO_3^- over $Cu_{0.5}Pd/Al_2O_3$ and $Sn_{0.5}Pd/Al_2O_3$ are plotted as a function of the logarithm of the initial NO_3^- concentrations ($[NO_3^-]_0$ = 0.4–1.6 mmol dm^{-3}). From the slopes, the reaction order with respect to NO_3^- was estimated, and from the reaction-order, the affinity for NO_3^- was estimated. Since the reaction order with respect to NO_3^- was 0.1 for $Sn_{0.5}Pd/Al_2O_3$ and 0.4 for $Cu_{0.5}Pd/Al_2O_3$, we concluded that the affinity of the Sn sites for NO_3^- was stronger than that of the Cu ones. The strong affinity of the Sn site for NO_3^- gives $Sn_{0.5}Pd/Al_2O_3$ a high tolerance against Cl^-, preventing a decrease in the catalytic activity in GW especially in the high conversion regions.

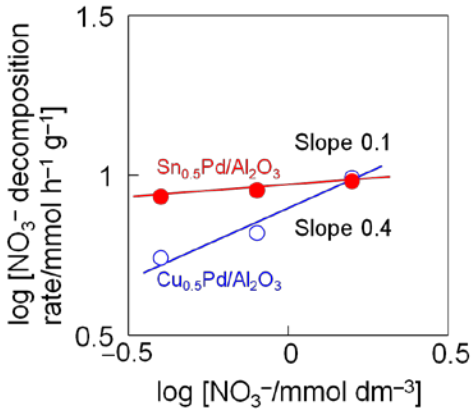

Figure 7 Dependencies of the NO_3^- decomposition rate on concentrations of NO_3^- over $Sn_{0.5}Pd/Al_2O_3$ (●) and $Cu_{0.5}Pd/Al_2O_3$ (○) for the catalytic hydrogenation of NO_3^- with H_2 in water. Reaction conditions: catalyst weight, 10 mg; reactant NO_3^- (from KNO_3), 0.4–1.6 mmol dm^{-3}; reaction volume, 250 cm^3; gas composition, H_2/CO_2 = 1/1; and gas flow rate, 30 cm^3 min^{-1}.

Conclusions

Tin-palladium supported on Al_2O_3, which had a Sn/Pd molar ratio of 0.5, showed high activity and high selectivity towards gaseous products (99%) for the hydrogenation of NO_3^- in aqueous NO_3^- solutions. Although the catalytic performances of both $Sn_{0.5}Pd/Al_2O_3$ and $Cu_{0.5}Pd/Al_2O_3$ decreased in groundwater, the decrease for $Sn_{0.5}Pd/Al_2O_3$ was less than that for $Cu_{0.5}Pd/Al_2O_3$. Nitrate in groundwater with 0.4 mmol dm^{-3} of NO_3^- (250 cm^3) was completely decomposed in 24 h at 298 K with a selectivity to gaseous products around 90% in the presence of $Sn_{0.5}Pd/Al_2O_3$. On the other hand, it took 60 h, and the selectivity to gaseous products was around 75% for $Cu_{0.5}Pd/Al_2O_3$. The insensitiveness to Cl^- and the strong affinity for NO_3^- of the Sn sites, which were estimated from adsorption isotherms of Cl^- and kinetic analysis of the hydrogenation of NO_3^-, lead to the superior catalytic performance of $Sn_{0.5}Pd/Al_2O_3$ in the groundwater.

Conflicts of interest

There are no conflicts to declare.

Acknowledgements

This work was supported by JSPS KAKENHI Grant Number 15J05423. We want to thank Dr. Osamu Tomita (Kyoto University) for his help in acquiring TEM images.

References

1 F. T. Wakida and D. N. Lerner, *Water Res.*, 2005, **39**, 3–16.
2 K. P. Cantor, *Cancer, Causes Control, Pap. Symp.*, 1997, **8**, 292–308.
3 WHO, *Guidelines for Drinking-Water Quality–First Addendum To the Third Edition;* World Health Organization, 2006.
4 K.-D. Vorlop and T. Tache, *Chem. Ing. Tech.*, 1989, **61**, 836–837.
5 F. Epron, F. Gauthard, J. Barbier and C. Pinéda, *J. Catal.*, 2001, **198**, 309–318.
6 F. Deganello, L. F. Liotta, A. Macaluso, A. M. Venezia and G. Deganello, *Appl. Catal., B,* 2000, **24**, 265–273.
7 I. Mikami, Y. Sakamoto, Y. Yoshinaga and T. Okuhara, *Appl. Catal., B,* 2003, **44**, 79–86.
8 J. Sá, S. Gross and H. Vinek, *Appl. Catal., A,* 2005, **294**, 226–234.
9 Y. Sakamoto, M. Kanno, T. Okuhara and Y. Kamiya, *Catal. Lett.*, 2008, 392–395.
10 F. Zhang, S. Miao, Y. Yang, X. Zhang, J. Chen and N. Guan, *J. Phys. Chem. C*, 2008, **112**, 7665–7671.
11 K. Wada, T. Hirata, S. Hosokawa, S. Iwamoto and M. Inoue, *Catal. Today*, 2012, **185**, 81–87.
12 Y. Yoshinaga, T. Akita, I. Mikami and T. Okuhara, *J. Catal.*, 2002, **207**, 37–45.
13 Y. Sakamoto, K. Nakamura, R. Kushibiki, Y. Kamiya and T. Okuhara, *Chem. Lett.*, 2005, **34**, 1510–1511.
14 A. E. Palomares, J. G. Prato, F. Márquez and A. Corma, *Appl. Catal., B,* 2003, **41**, 3–13.
15 N. Barrabés, J. Just, A. Dafinov, F. Medina, J. L. G. Fierro, J. E. Sueiras, P. Salagre and Y. Cesteros, *Appl. Catal., B,* 2006, **62**, 77–85.
16 J. Sá, N. Barrabé, E. Kleymenov, C. Lin, K. Föttinger, O. V. Safonova, J. Szlachetko, J. A. Bokhoven, M. Nachtegaal, A. Urakawa, G. A. Crespof and G. Rupprechter, *Catal. Sci. Technol.*, 2012, **2**, 794–799.
17 W. Gao, N. Guan, J. Chen, X. Guan, R. Jin, H. Zeng, Z. Liu and F. Zhang, *Appl. Catal., B,* **2003**, 46, 341–351.
18 S. Hamid, S. Bae, W. Lee, M. T. Amin and A. A. Alazba, *Ind. Eng. Chem. Res.*, 2015, **54**, 6247−6257.
19 A. Garron and F. Epron, *Water Res.*, 2005, **39**, 3073–3081.
20 I. Dodouche, D. P. Barbosa, M. d. C. Rangel and F. Epron, *Appl. Catal., B,* 2009, **93**, 50−55.
21 Z. Luo, M. Ibáñez, A. M. Antolín, A. Genç, A. Shavel, S. Contreras, F. Medina, J. Arbiol and A. Cabot, *Langmuir*, 2015, **31**, 3952−3957.
22 S. Hamid, M. A. Kumar and W. Lee, *Appl. Catal., B,* 2016, **187**, 37–46.
23 A. E. Palomares, C. Franch and A. Corma, *Catal. Today*, 2011, **172**, 90–94.
24 U. Prüsse and K.-D. Vorlop, *J. Mol. Catal., A,* 2001, **173**, *313–328.*
25 R. Zhang, D. Shuai, K. A. Guy, J. R. Shapley, T. J. Strathmann and C. J. Werth, *ChemCatChem*, 2013, **5**, 313–321.
26 Z. Gao, Y. Zhang, D. Li, C. J. Werth, Y. Zhang and X. Zhou, *J. Hazard. Mater.*, 2015, **286**, 425−431.
27 A. H. Pizarro, C. B. Molina, J. J. Rodriguez and F. Epron, *J. Environ. Chem. Eng.*, 2015, **3**, 2777−2785.
28 M. Al Bahri, L. Calvo, M. A. Gilarranz, J. J. Rodriguez, and F. Epron, *Appl. Catal., B,* 2013, **138**, 141.
29 A. Pintar, M. Šetinc, and J. Levec, *J. Catal.*, 1998, **174**, 72–87.
30 A. E. Palomares, C. Franch, and A. Corma, *Catal. Today*, 2010, **149**, 348–351.
31 Y. Wang, Y. Sakamoto, and Y. Kamiya, *Appl. Catal., A,* 2009, **361**, 123–129.
32 B. P. Chaplin, E. Roundy, K. A. Guy, J. R. Shapley and C. J. Werth, *Environ. Sci. Technol.*, 2006, **40**, 3075−3081.

33 O. S. G. P. Soares, J. J. M. Ó rfa, E. Gallegos-Suarez, E. Castillejos, I. Rodríguez-Ramos and M. F. R. Pereira, *Environ. Technol.* 2012, **33**, 2353−2358.
34 J. Hirayama and Y. Kamiya, *ACS Catal.*, 2014, **4**, 2207−2215.
35 U. Prüsse, M. Hähnlein, J. Daum and K.-D. Vorlop, *Catal. Today*, 2000, **55**, 79–90.
36 C. Franch, E. Rodríguez-Castellón, A. Reyes-Carmona and A. E. Palomares, *Appl. Catal., A*, 2012, **425−426**, 145−152.
37 Y. Wang, J. Qu and H. Liu, *J. Mol. Catal., A*, 2007, **272**, 31−37.
38 J. Martiínez, A. Ortiz and I. Ortiz, *Appl. Catal., B*, 2017, **207**, 42−59.
39 C. L. Constantinou, C. N. Costa and A. M. Efstathiou, *Catal. Today*, 2010, **151**, 190−194.
40 A. Pintar, J. Batista, J. Levec and T. Kajiuchi, *Appl. Catal., B*, 1996, **11**, 81−98.
41 C. L. Constantinou, C. N. Costa and A. M. Efstathiou, *Environ. Sci. Technol.*, 2007, **41**, 950−956.
42 A. E. Palomares, J. G. Prato, F. Rey and A. Corma, *J. Catal.*, 2004, **221**, 62−66.
43 P. Canton, G. Fagherazzi, M. Battagliarin, F. Menegazzo, F. Pinna and N. Pernicon, *Langmuir*, 2002, **18**, 6530−6535.